# Chain Stiffness and Excluded-Volume Effects in Dilute Polymer Solutions: Cellulose Tris[(3,5-Dimethylphenyl)carbamate]

**Akihiko Tsuboi, Takashi Norisuye,* and Akio Teramoto**

*Department of Macromolecular Science, Osaka University, Toyonaka, Osaka 560, Japan*

*Received September 8, 1995; Revised Manuscript Received December 21, 1995*[⊗]

ABSTRACT: Nineteen fractions of cellulose tris[(3,5-dimethylphenyl)carbamate] (CTDC) ranging in weight-average molecular weight $M_w$ from $2.5 \times 10^4$ to $7.5 \times 10^6$ have been studied by static light scattering, sedimentation equilibrium, and viscometry in 1-methyl-2-pyrrolidone at 25 °C. Since this cellulose derivative exhibits pronounced optical anisotropy, light-scattering data are corrected for the anisotropy effect on the basis of Nagai theory for the Kratky−Porod (KP) wormlike chain with cylindrically symmetric polarizabilities. It is shown that the data for $\langle S^2\rangle_z$ (the *z*-average mean-square radius of gyration), $\delta$ (the optical anisotropy factor), and $[\eta]$ (the intrinsic viscosity) and those reported previously for 11 fractions are described accurately by the known theories for the unperturbed KP chain if $M_w$ is lower than $7 \times 10^5$. From the comparison, the persistence length and the monomeric projection of the CTDC chain are estimated to be 7.8 and 0.52 nm, respectively. When $M_w$ exceeds $10^6$, i.e., when $n_K$ (the Kuhn segment number) increases above 50, excluded-volume effects on $\langle S^2\rangle_z$ and $[\eta]$ become experimentally observable. Though such a large $n_K$ value for the appearance of volume effects has been considered inconsistent with the Yamakawa−Stockmayer−Shimada (YSS) theory for KP or helical wormlike chains, the observed excluded-volume effects are found to be explained quantitatively in the YSS scheme, i.e., by the YSS perturbation theory combined with the Domb−Barrett function for the radius expansion factor and the Barrett function for the viscosity expansion factor. Thus, this theoretical scheme should have a wider applicability than what might be anticipated from earlier studies.

## Introduction

Excluded-volume effects on the dimensional and hydrodynamic properties of a semiflexible polymer in a nonideal solvent should become experimentally observable when the molecular weight $M$ exceeds a certain value. By analyzing available data for the mean-square radius of gyration $\langle S^2\rangle$ on the basis of the Kratky−Porod (KP) wormlike chain,[1] Norisuye and Fujita[2] estimated the Kuhn segment number $n_K$ for such an onset of volume effect to be about 50. This $n_K$ value has since served as an empirical guide for the molecular characterization of semiflexible polymers based on the unperturbed KP model, i.e., for experimental determination of the persistence length and the linear mass density.

However, Norisuye and Fujita's finding raised a very fundamental problem that still remains unsolved,[3] in that the estimated $n_K$ value (or more generally the ratio of the contour length to the stiffness parameter in the helical wormlike chain[4]) was 1 order of magnitude larger than that predictable from the Yamakawa−Stockmayer−Shimada (YSS) perturbation theory[5−7] for KP or helical wormlike chains. In other words, intramolecular volume exclusion in actual semiflexible polymers appeared to be suppressed more strongly than predicted by this theory. Yamakawa and Shimada[6] examined the discrepancy by comparing theoretical and experimental $\langle S^2\rangle$ and concluded that the YSS scheme (i.e., the YSS theory combined with the Domb−Barrett function[8] for the radius expansion factor), which is now known to be valid for flexible chains,[9−13] breaks down for poly(hexyl isocyanate), a typical stiff chain. This conclusion may suggest need of reconsideration of the YSS theory for polymers with high stiffness, but since it is based on the $\langle S^2\rangle$ data for one particular polymer + solvent system,[14] further experimental study with other stiff polymers, preferably on both $\langle S^2\rangle$ and $[\eta]$ (the intrinsic viscosity), is needed. Such work must cover an $M$ range broad enough to allow not only unequivocal determination of the model parameters for the unperturbed KP or helical wormlike chain in a region of low $M$ but also observation of intramolecular excluded-volume effects at high $M$. Only a few available data of $\langle S^2\rangle$ and $[\eta]$ for stiff polymers satisfy these conditions.

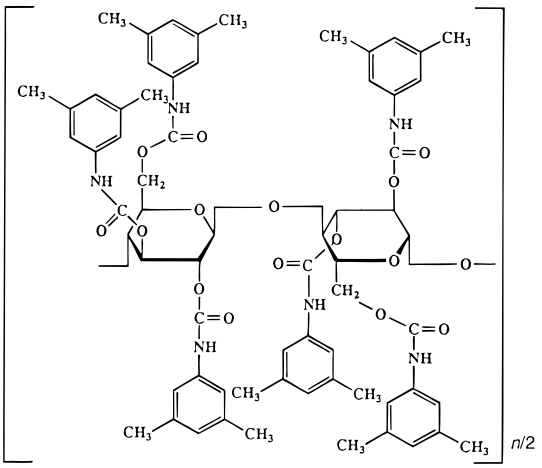

**Figure 1.** Chemical structure of cellulose tris[(3,5-dimethylphenyl)carbamate] (CTDC).

In our recent characterization work[15] by light scattering and viscometry, it was found that cellulose tris[(3,5-dimethylphenyl)carbamate] (CTDC), whose chemical structure is shown in Figure 1, behaves like an unperturbed KP chain in 1-methyl-2-pyrrolidone (or *N*-methyl-2-pyrrolidone, NMP) at 25 °C but tends to undergo intramolecular excluded-volume effects when the weight-average molecular weight $M_w$ exceeds $10^6$. The persistence length estimated was 7.8 nm, indicating a considerable stiffness of the CTDC chain. Further, our previous work showed that narrow-distribution fractions could be prepared by extensive fractionation. Thus, we expected this cellulose derivative to be useful for exploring excluded-volume effects in semiflexible polymer solutions and made light-scattering and viscos-

[⊗] Abstract published in *Advance ACS Abstracts,* April 1, 1996.

S0024-9297(95)01344-1 CCC: $12.00 

ity measurements on CTDC fractions covering in $M_w$ from $2.5 \times 10^4$ to $7.5 \times 10^6$ with NMP at 25 °C as the solvent. In the work reported below, the data of $\langle S^2\rangle_z$ (the *z*-average $\langle S^2\rangle$) and $[\eta]$ obtained are analyzed along with our previous results on the basis of the KP model to determine the model parameters characterizing the CTDC chain in the unperturbed state, and then excluded-volume effects on the measured $\langle S^2\rangle_z$ and $[\eta]$ at high $M_w$ are compared with predictions from the YSS theory.

## Experimental Section

**Samples.** Fully substituted samples of CTDC were previously[15] prepared by the reaction of cellulose with 3,5-dimethylphenyl isocyanate in pyridine at 140−150 °C followed by repeated fractional precipitation with NMP as the solvent and methanol as the precipitant. From these, 19 middle fractions were chosen for the present study. Their molecular weights were determined by light scattering or sedimentation equilibrium in NMP at 25 °C. NMP was dehydrated with calcium hydride and fractionally distilled under reduced nitrogen atmosphere just before use.

**Light Scattering.** Intensities of light scattered from CTDC in NMP at 25 °C were measured on a Fica 50 light-scattering photometer using vertically polarized incident light of 436 or 546 nm wavelength. In all actual experiments for the former wavelength, however, a 436 nm filter was placed in front of the photomultiplier to minimize possible fluorescence contributions to light-scattering intensities. The measurement was also made for the depolarized component, with an analyzer set in the horizontal direction, since the CTDC chain was optically anisotropic. For its specific refractive index increment at 25 °C, the previously determined values[15] of 0.105 $cm^3\ g^{-1}$ for 436 nm and 0.0966 $cm^3\ g^{-1}$ for 546 nm were used. Test solutions and NMP were made optically clean by filtration through a Millipore filter followed by centrifugation at about $(4 \times 10^4)g$ for 2 h (Sorval RC-5C).

The apparatus was calibrated with pure benzene at 25 °C as the reference liquid. The Rayleigh ratio of this liquid for unpolarized light was taken to be 46.5 and 16.1 $cm^{-1}$ for 436 and 546 nm, respectively. Its depolarization ratio was determined to be 0.40 for both wavelengths by the method of Rubingh and Yu.[16]

The scattering intensity data obtained as functions of scattering angle $\theta$ and polymer mass concentration $c$ were analyzed according to the equations[17−19]

$$\lim_{c\to 0}(Kc/R_{\theta,\mathrm{U_v}})^{1/2} = M_{\mathrm{w,app}}{}^{-1/2}[1 + {}^1/_6(4\pi n_0/\lambda_0)^2\langle S^2\rangle_{\mathrm{z,app}}\sin^2(\theta/2) + ...] \quad (1a)$$

$$\lim_{\theta\to 0}(Kc/R_{\theta,\mathrm{U_v}})^{1/2} = M_{\mathrm{w,app}}{}^{-1/2} + A_{2,\mathrm{app}}M_{\mathrm{w,app}}{}^{1/2}c + ... \quad (1b)$$

$$\lim_{\substack{\theta\to 0\\ c\to 0}} R_{\theta,\mathrm{H_v}}/R_{\theta,\mathrm{U_v}} = 3\delta/(1 + 7\delta) \quad (2)$$

where

$$M_{\mathrm{w,app}} = M_w(1 + 7\delta) \quad (3)$$

$$\langle S^2\rangle_{\mathrm{z,app}} = \langle S^2\rangle^*/(1 + 7\delta) \quad (4)$$

$$A_{2,\mathrm{app}} = A_2/(1 + 7\delta)^2 \quad (5)$$

In these equations, $K$ is the optical constant, $R_{\theta,\mathrm{U_v}}$ and $R_{\theta,\mathrm{H_v}}$ are the reduced scattering intensities at $\theta$ for vertically polarized incident light without analyzer and with analyzer in the horizontal direction, respectively, $M_{\mathrm{w,app}}$, $\langle S^2\rangle_{\mathrm{z,app}}$, and $A_{2,\mathrm{app}}$ are the apparent values of $M_w$, $\langle S^2\rangle_z$, and $A_2$ (the second virial coefficient), respectively, $n_0$ is the refractive index of the solvent, $\lambda_0$ is the wavelength of incident light in vacuum, $\delta$ is the optical anisotropy factor, and $\langle S^2\rangle^*$ is an apparent mean-square radius of gyration. It should be noted that except for Gaussian chains, $\langle S^2\rangle^*$ differs from the true $\langle S^2\rangle_z$ unless $\delta = 0$.[19,20]

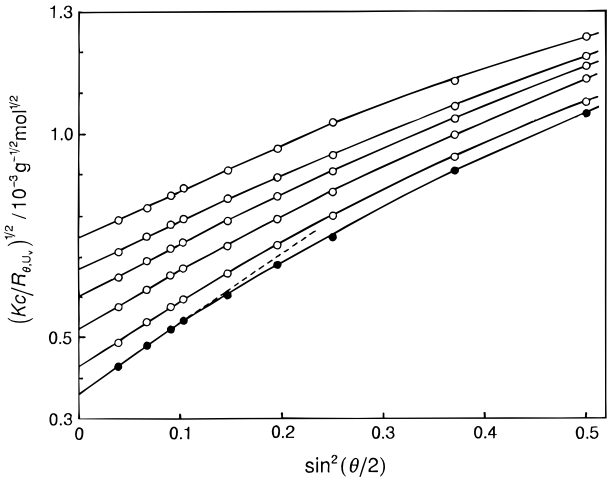


**Figure 2.** Angular dependence of $(Kc/R_{\theta,\mathrm{U_v}})^{1/2}$ at different polymer concentrations for CTDC sample M8 in NMP at 25 °C and 546 nm. The polymer concentrations in units of $10^{-3}$ g $cm^{-3}$ are 1.714, 1.308, 0.9981, 0.6553, 0.3114, and 0 (●) from top to bottom. The dashed line indicates the initial slope.

**Ultracentrifugation.** Sedimentation equilibrium measurements were made on four samples of relatively low molecular weights in NMP at 25 °C. Use was made of a Beckman Model E ultracentrifuge with a Kel-F 12 mm double-sector cell. The liquid column was adjusted to 1.2−1.5 mm, and the rotor speed was chosen to be $(9 \times 10^3)$−$(2.6 \times 10^4)$ rpm depending on the sample's molecular weight. The partial specific volume of CTDC in NMP at 25 °C was taken to be 0.782 $cm^3\ g^{-1}$.[15] Values of $M_z/M_w$ (the *z*-average to weight-average molecular weight ratio) were also determined for three of the samples by analyzing the equilibrium concentration profiles in the manner described previously;[15] that for one sample (designated T260) could not be estimated owing to remarkable nonideality.

**Viscometry.** Zero-shear intrinsic viscosities in NMP at 25 °C were determined using a four-bulb low-shear capillary viscometer (apparent shear rates of 8−56 $s^{-1}$ for pure NMP at 25 °C) for the three highest molecular weight samples and conventional capillary viscometers of the Ubbelohde type for the rest. For samples with $[\eta] < 50$ $cm^3\ g^{-1}$, the relative viscosity was evaluated by taking account of the difference between the solvent and solution densities.

## Results and Discussion

**Results from Light Scattering and Sedimentation Equilibrium.** Figure 2 illustrates the angular dependence of $(Kc/R_{\theta,\mathrm{U_v}})^{1/2}$ at different polymer concentrations for CTDC sample M8, the highest molecular weight studied. The filled circles represent the infinite dilution values of $(Kc/R_{\theta,\mathrm{U_v}})^{1/2}$ and the dashed line the initial slope of the curve fitting them.

The values of $M_w$, $A_2$, $\delta$, and $\langle S^2\rangle^*$ determined according to eqs 1−5 are summarized in Table 1, along with those of $M_w$, $A_2$, and $M_z/M_w$ obtained from sedimentation equilibrium. The values of $M_z/M_w$ indicate that samples T92, T37, and T25 are fairly narrow in molecular weight distribution, as was previously shown to be the case for some other CTDC samples.[15] The data of $\delta$ as a function of $M_w$ are shown in Figure 3, in which our previous data[15] (the circles with pip) are also included. The two data sets are fitted essentially by a single curve, whose slope is about −1 for $M_w$ above $10^5$. Though not shown here, the previous and present data for $\langle S^2\rangle^*$ are also consistent with each other. Note that to evaluate $\langle S^2\rangle_z$ from $\langle S^2\rangle^*$, a suitable model must be assumed.[19,20]

**Table 1. Results from Light-Scattering and Sedimentation Equilibrium Measurements on CTDC Samples in NMP at 25 °C**

| sample | $10^{-4}M_w$ | $10^4A_2$, mol g$^{-2}$ cm$^{-3}$ | $10^3\delta$ | $M_z/M_w$ | $10^{12}\langle S^2\rangle^*$, cm$^2$ | $10^{12}\langle S^2\rangle_z$, cm$^2$ |
|---|---|---|---|---|---|---|
| M8 | 751 | 0.854 | | | 241 | 241 |
| M6 | 610 | 0.921 | | | 181 | 181 |
| M4a | 427 | 1.06 | | | 120 | 120 |
| M1a | 144 | 1.42 | 0.8 | | 37.3 | 37.2 |
| M1b | 103 | 1.84 | 0.9 | | 25.2 | 25.1 |
| T660 | 65.9 | 2.09 | 1.6 | | 15.2 | 15.1 |
| T460 | 45.7 | 2.34 | 2.0 | | 10.6 | 10.5 |
| T390 | 38.5 | 2.21 | 2.3 | | 8.79 | 8.65 |
| T300 | 29.5 | 2.65 | 3.3 | | 6.77 | 6.63 |
| T260 | 26.3[a] | 2.82[a] | | | | |
| T210 | 21.0 | 2.98 | 4.1 | | 4.76 | 4.62 |
| T150 | 14.8 | 4.03 | 6.7 | | 3.14 | 3.00 |
| T120 | 12.2 | 3.76 | 7.3 | | 2.56 | 2.42 |
| T92 | 9.21[a] | 5.27[a] | | 1.1[a] | | |
| T56 | 5.55 | 4.55 | 18 | | | |
| T52 | 5.17 | 4.80 | 19 | | | |
| T46 | 4.57 | 5.59 | 20 | | | |
| T37 | 3.68[a] | 6.50[a] | | 1.1[a] | | |
| T25 | 2.48[a] | 5.50[a] | | 1.1[a] | | |

[a] From sedimentation equilibrium.

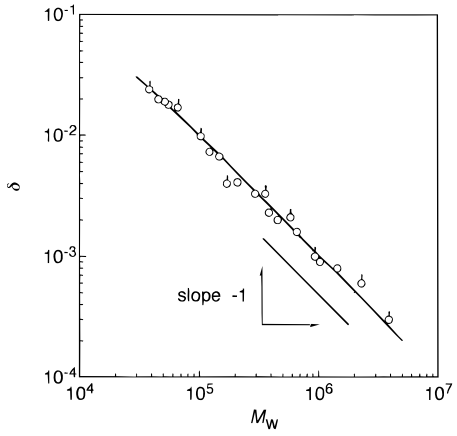


**Figure 3.** Molecular weight dependence of optical anisotropy factor for CTDC in NMP at 25 °C. Our previous data[15] are indicated by circles with pip. The curve represents the theoretical values calculated from eq 7 with $q = 7.8$ nm, $M_L = 1080$ nm$^{-1}$, $|\epsilon| = 2.85$ (see the text). Its slope is about $-1$ for molecular weights above $10^5$.

**Determination of True Radii of Gyration.** As in our previous work,[15] we model the CTDC molecule in NMP by the KP chain with cylindrically symmetric polarizabilities. The unperturbed mean-square radius of gyration $\langle S^2\rangle_0$ and $\delta$ of this chain with contour length $L$ and persistence length $q$ are given by[19,21]

$$\langle S^2\rangle_0 = (qL/3) - q^2 + (2q^3/L) - (2q^4/L^2)[1 - \exp(-L/q)] \quad (6)$$

$$\delta = (2\epsilon^2 q/135L)\{1 - (q/3L)[1 - \exp(-3L/q)]\} \quad (7)$$

Here, $\epsilon$ is the polarizability parameter defined by $3(\alpha_1 - \alpha_2)/(\alpha_1 + 2\alpha_2)$, with $\alpha_1$ and $\alpha_2$ being the longitudinal and transverse polarizabilities per unit contour length, but its value derived directly from the measured (total) $R_{\theta,H_v}/c$ at zero angle and infinite dilution is only apparent because $R_{\theta,H_v}$ generally contains a substantial contribution from the collision-induced component[22−24] and also because $\epsilon$ in solution is subjected to the effect of internal field;[25] correction for these factors can lower $|\epsilon|$ by a factor of 2. In the ensuing analysis, we regard $\epsilon$ as an adjustable parameter independent of molecular weight.

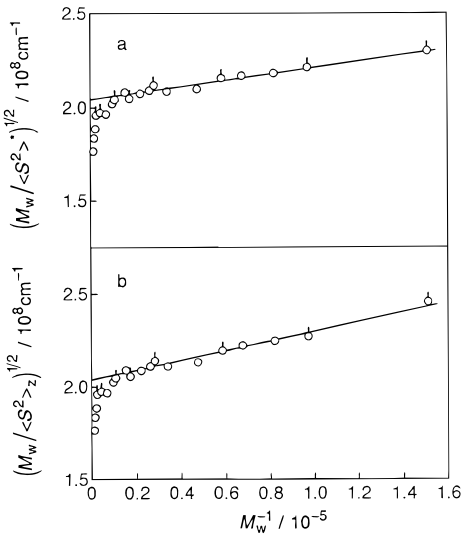


**Figure 4.** Plots of $(M_w/\langle S^2\rangle^*)^{1/2}$ vs $M_w^{-1}$ (a) and $(M_w/\langle S^2\rangle_z)^{1/2}$ vs $M_w^{-1}$ (b) for CTDC in NMP at 25 °C. Circles with pip, previous data.[15]

Equation 6 can be approximated by[14]

$$(M/\langle S^2\rangle_0)^{1/2} = (3M_L/q)^{1/2} + q^{1/2}(3M_L)^{3/2}/(2M) \quad (8)$$

provided that $n_K$ ($=L/2q$) > 2. Here, $M_L$ is the molar mass per unit contour length defined by $M_L = M/L$. Under the same condition for $n_K$, Nagai's theory[19] for $\langle S^2\rangle^*$ is written in a good approximation as[26]

$$\langle S^2\rangle^* = \langle S^2\rangle_0 - f_{U_v} \quad (9)$$

with

$$f_{U_v} = (4q^2/45)\{\epsilon[1 - (8qM_L/3M) + (26q^2M_L^2/9M^2)] - (23\epsilon^2 qM_L/126M)[(1 - (103qM_L/69M)]\} \quad (10)$$

These equations indicate that the three parameters $q$, $M_L$, and $\epsilon$ must be known in order to evaluate the true $\langle S^2\rangle_z$ from $\langle S^2\rangle^*$ data. As in our previous work,[15] we determined these parameters and $\langle S^2\rangle_z$ simultaneously from the data of $\langle S^2\rangle^*$, $\delta$, and $M_w$ in Table 1 by the following iteration method.[26]

First, approximate values of $M_L$ and $q$ were estimated from the intercept and slope of the $(M_w/\langle S^2\rangle^*)^{1/2}$ vs $M_w^{-1}$ plot constructed in Figure 4a according to eq 8 with $\langle S^2\rangle_0$ replaced by $\langle S^2\rangle^*$; the pronounced downward deviations of the six plotted points at small $M_w^{-1}$ may be ascribed to excluded-volume effects on $\langle S^2\rangle$. The first approximate values of $M_L$ and $q$ were then used to find $\epsilon$ which allows eq 7 to best fit the experimental $\delta$ vs $M_w$ relation in Figure 3; $\epsilon$ for CTDC was taken to be negative on the basis of flow birefringence data[27,28] for cellulose tris(phenylcarbamate) in various solvents. With the values of $M_L$, $q$, and $\epsilon$ thus estimated, $f_{U_v}$ in eq 10 was calculated to obtain first-approximate values of $\langle S^2\rangle_z$ as a function of $M_w$. On iterating this procedure twice, we reached the following convergent parameter values: $q = 7.8$ ($\pm$0.6) nm, $M_L = 1080$ ($\pm$60) nm$^{-1}$, and $\epsilon = -2.85$ ($\pm$0.2) (the values of $\langle S^2\rangle_z$ are presented in the last column of Table 1). The curve in Figure 3 actually represents the $\delta$ values calculated from eq 7 with these parameter values, and Figure 4b shows the $(M_w/\langle S^2\rangle_z)^{1/2}$

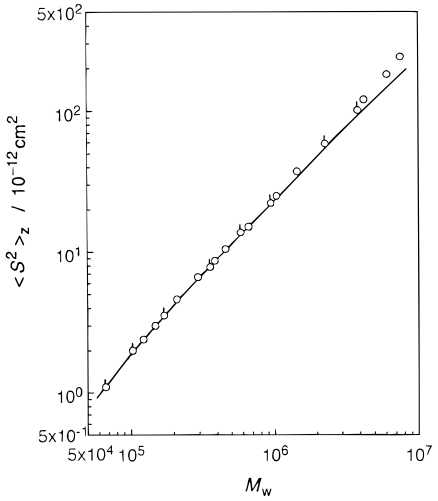


**Figure 5.** Experimental $\langle S^2\rangle_z$ for CTDC in NMP at 25 °C compared with the theoretical curve (eq 6) for the unperturbed wormlike chain with $q = 7.8$ nm and $M_L = 1080$ nm$^{-1}$. Circles with pip, previous data.[15]

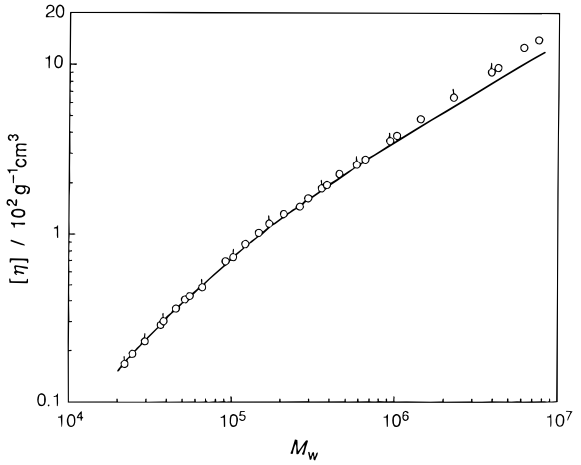


**Figure 6.** Molecular weight dependence of $[\eta]$ for CTDC in NMP at 25 °C. Our previous data[15] are distinguished by pip. The curve represents the theoretical values calculated from the theory of Yoshizaki et al.[29] for the unperturbed wormlike touched-bead chain with $q = 7.8$ nm, $M_L = 1140$ nm$^{-1}$, and $d_b = 3.9$ nm.

vs $M_w^{-1}$ plot in the final step. The values of $q$ and $M_L$ determined here are identical with those estimated previously from limited data (our previous $\epsilon$ value was $-2.9$). If correction for polydispersity is made with $M_z/M_w = 1.1$ (see Table 1 and also ref 15), the present $M_L$ and $\epsilon$ values are replaced by 1190 nm$^{-1}$ and $-2.7$, respectively, while $q$ remains almost unchanged. Note that for a not-too-broad sample, $M_L$ in eq 8 may be replaced with $M_L(M_w/M_z)$ in a first approximation and also that $\delta$ is essentially free from the polydispersity effect since it is almost proportional to $M_w^{-1}$ in our molecular weight range.

Figure 5 shows that the previous and present $\langle S^2\rangle_z$ data for $M_w$ below $10^6$ are closely fitted by the theoretical curve computed from eq 6 with $q = 7.8$ nm and $M_L = 1080$ nm$^{-1}$. For $M_w$ above $10^6$, the plotted points deviate upward progressively with increasing $M_w$, confirming our previous finding from limited data (for $M_w < 4 \times 10^6$) that excluded-volume effects on $\langle S^2\rangle_z$ of CTDC become observable when $M_w$ exceeds about $10^6$. We note that in this high $M_w$ region, the data points approximately follow a straight line with slope 1.1 (not shown here), while the theoretical curve has a slope of about unity.

**Intrinsic Viscosity.** The results for $[\eta]$ and Huggins' constant $k'$ are presented in Table 2, and the vlaues of $[\eta]$ are plotted double-logarithmically against $M_w$ in Figure 6, along with our previous data.[15] The viscosity exponent is about 0.95 for $M_w < 10^5$ and 0.66 for $M_w > 2 \times 10^5$. The curve in the figure represents the theoretical values calculated from the theory of Yoshizaki, Nitta, and Yamakawa[29] for $[\eta]_0$ of an unperturbed KP touched-bead chain using the previously estimated parameters:[15] $q = 7.8$ nm, $M_L = 1140$ nm$^{-1}$, and $d_b$ (the hydrodynamic bead diameter) $= 3.9$ nm; we note that the $q$ value from $\langle S^2\rangle_z$ was previously assumed to be applicable to $[\eta]$ since the three parameters could not uniquely be determined from the $[\eta]$ data. The agreement between theory and experiment is seen to be good for $M_w < 7 \times 10^5$ (hence it is unnecessary to redetermine the model parameters characterizing $[\eta]_0$ of the CTDC chain). The $M_L$ values of 1190 and 1140 nm$^{-1}$ from $\langle S^2\rangle$ (polydispersity-corrected) and $[\eta]$, respectively, are also in substantial agreement. These findings allow us to conclude that in the region of $M_w$ below $7 \times 10^5$, the molecular weight dependences of $\langle S^2\rangle_z$, $\delta$, and $[\eta]$ are explained consistently by the known theories[19,21,29] for the unperturbed KP chain.

**Table 2. Results from Viscosity Measurements on CTDC Samples in NMP at 25 °C.**

| sample | $[\eta]10^{-2}$, cm$^3$ g$^{-1}$ | $k'$ |
|---|---|---|
| M8 | 14.0 | 0.33 |
| M6 | 12.6 | 0.34 |
| M4a | 9.64 | 0.33 |
| M1a | 4.79 | 0.31 |
| M1b | 3.82 | 0.38 |
| T660 | 2.73 | 0.37 |
| T460 | 2.26 | 0.35 |
| T390 | 1.95 | 0.38 |
| T300 | 1.63 | 0.43 |
| T260 | 1.45 | 0.34 |
| T210 | 1.31 | 0.37 |
| T150 | 1.02 | 0.32 |
| T120 | 0.876 | 0.39 |
| T92 | 0.693 | 0.40 |
| T56 | 0.428 | 0.40 |
| T52 | 0.408 | 0.45 |
| T46 | 0.359 | 0.35 |
| T37 | 0.286 | 0.39 |
| T25 | 0.191 | 0.45 |

The $M_L$ values of 1190 and 1140 nm$^{-1}$ with the molar mass of 603.7 per residue yield 0.52 ($\pm$0.01) nm for the monomeric projection along the chain contour of the CTDC chain. This monomeric length is quite close to the literature values of 0.51−0.52 nm for cellulose[30] and its derivatives[31,32] in the crystalline state, confirming that the KP chain is an excellent model for CTDC in NMP. The bead diameter of 3.9 nm based on the theory of Yoshizaki et al.[29] corresponds to a cylinder diameter of 2.9 nm (in the Yamakawa−Fujii−Yoshizaki theory for KP cylinders[33,34]), which is only slightly larger than the maximal diameter estimated from the chemical structure of CTDC (to account for the difference, solvation of NMP molecules onto the polymer chain may have to be considered).

As can be seen in Figure 6, excluded-volume effects on $[\eta]$ become experimentally detectable at $M_w = 7 \times 10^5$−$10^6$, being consistent with the finding on $\langle S^2\rangle_z$ in Figure 5. The molecular weight of $7 \times 10^5$−$10^6$ for this onset of volume effect corresponds to an $n_K$ of 40−50, which is comparable to Norisuye and Fujita's estimate[2] mentioned in the Introduction. The question is whether

the YSS theory[5−7] is capable of explaining the volume effects which appear to be negligibly small for $n_K < 40$ but appreciable for $n_K > 50$. The check of this point is the core of the present work.

**Excluded-Volume Effects.** In the YSS scheme[5−7] for KP or helical wormlike (HW) chains, the radius expansion factor $\alpha_S$ [$\equiv(\langle S^2\rangle/\langle S^2\rangle_0)^{1/2}$] and the viscosity expansion factor $\alpha_\eta$ [$\equiv([\eta]/[\eta]_0)^{1/3}$] are universal functions of the scaled excluded-volume parameter $\tilde{z}$ defined by

$$\tilde{z} = {}^3/_4 K(\lambda L) z \tag{11}$$

with

$$\begin{aligned} K(\lambda L) &= {}^4/_3 - 2.711(\lambda L)^{-1/2} + {}^7/_6(\lambda L)^{-1} \quad \text{for } \lambda L > 6 \\ &= (\lambda L)^{-1/2} \exp[-6.611(\lambda L)^{-1} + 0.9198 + \\ &\qquad 0.03516\lambda L] \quad \text{for } \lambda L \le 6 \end{aligned} \tag{12}$$

and

$$z = (3/2\pi)^{3/2}(\lambda B)(\lambda L)^{1/2} \tag{13}$$

Here, $\lambda^{-1}$ is the stiffness parameter, $z$ is the conventional excluded-volume parameter, and $B$ is the excluded-volume strength representing the interaction between a pair of beads. The KP chain, with which we are concerned here, is a special case of the HW chain,[4] and in this case, there hold the relations

$$\lambda^{-1} = 2q \qquad \text{(KP)} \tag{14}$$

$$B = \beta/a^2 \qquad \text{(KP)} \tag{15}$$

with $\beta$ and $a$ being the binary cluster integral and the bead spacing, respectively. Note that $\lambda L = n_K$ in the KP limit of the HW chain.

Following Yamakawa and co-workers,[6,11] we adopt the Domb−Barrett function[8] for $\alpha_S^2$ and the Barrett function[35] for $\alpha_\eta^3$, with $z$ replaced by $\tilde{z}$:

$$\alpha_S^{\,2} = \left[1 + 10\tilde{z} + \left(\frac{70\pi}{9} + \frac{10}{3}\right)\tilde{z}^2 + 8\pi^{3/2}\tilde{z}^3\right]^{2/15} \times [0.933 + 0.067\exp(-0.85\tilde{z} - 1.39\tilde{z}^2)] \tag{16}$$

$$\alpha_\eta^{\,3} = (1 + 3.8\tilde{z} + 1.9\tilde{z}^2)^{0.3} \tag{17}$$

These equations accurately describe experimental data for flexible polymers[9−13] with $\lambda^{-1}$ of 1.3−5.8 nm over a very broad range of molecular weight and also for sodium hyaluronate[36] with $\lambda^{-1} = 8.2$ nm ($q = 4.1$ nm) in aqueous NaCl at high ionic strength. As may be seen from eqs 11−17, $B$ is the only unknown necessary for the theoretical evaluation of $\alpha_S^2$ and $\alpha_\eta^3$ (and hence of $\langle S^2\rangle$ and $[\eta]$) for CTDC since all the other parameters are known.

In Figure 7, our $\langle S^2\rangle_z$ data are compared with the theoretical values (the solid curve) calculated from eqs 6 and 16 with $q = 7.8$ nm, $M_L = 1080$ nm$^{-1}$, and $B = 0.50$ nm. The agreement is satisfactory throughout the entire range of molecular weight studied. The dashed line in the figure represents the theoretical values for the unperturbed KP chain with the same $q$ and $M_L$ values. Importantly, the difference between the solid and dashed lines remains small up to $M \sim 6.6 \times 10^5$ (i.e., $n_K \sim 40$), being at most 5%.

A similar comparison for $[\eta]$ is shown in Figure 8, in which the solid curve represents the theoretical values

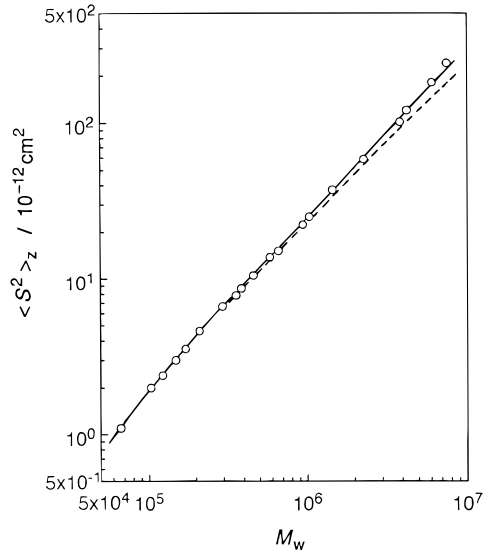


**Figure 7.** Comparison between the measured $\langle S^2\rangle_z$ for CTDC in NMP and the YSS theoretical values (solid line) calculated from eqs 6 and 16 with $q = 7.8$ nm, $M_L = 1080$ nm$^{-1}$, and $B = 0.5$ nm. Dashed line, theoretical values for $B = 0$.

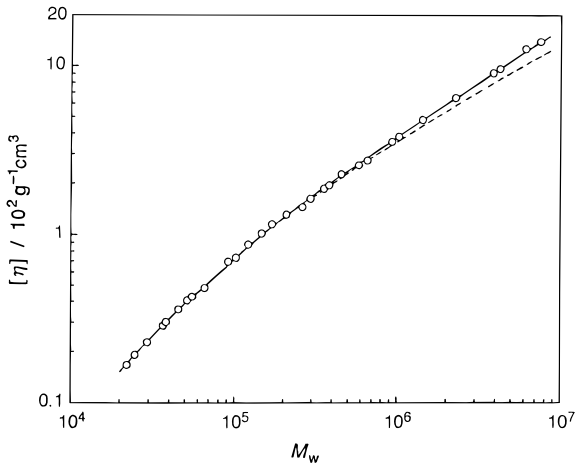


**Figure 8.** Comparison of the measured $[\eta]$ for CTDC in NMP with the YSS theoretical values (solid curve) for $q = 7.8$ nm, $M_L = 1140$ nm$^{-1}$, and $d_b = 3.9$ nm. Dashed line, theoretical values for $B = 0$.

for the perturbed KP chain with $q = 7.8$ nm, $M_L = 1140$ nm$^{-1}$, $d_b = 3.9$ nm, and $B = 0.50$ nm, while the dashed one again refers to the unperturbed state. It can be seen that the solid line closely fits the data points over the entire molecular weight range. This line stays close to the unperturbed line for $M$ below $6.6 \times 10^5$ (the difference is only 5% at $M = 6.6 \times 10^5$), as is the case for $\langle S^2\rangle$. We may therefore conclude that the YSS scheme quantitatively explains the substantially unperturbed behavior of the CTDC chain for $n_K$ below 40 and the appreciable excluded-volume effects on its $\langle S^2\rangle_z$ and $[\eta]$ for $n_K$ above 50. This reconciles the YSS theory with Norisuye and Fujita's finding[2] (on stiff chains) that volume effects on $\langle S^2\rangle_z$ become experimentally visible at $n_K \sim 50$. The point is that below $n_K \sim 40$, the theoretically predicted volume effects in the CTDC chain are too small to be observed by experiment as upward deviations of $\langle S^2\rangle_z$ and $[\eta]$ from the unperturbed lines.

The $B$ value of 0.50 nm for the CTDC chain is comparable to those for flexible polymers[9,10,13,37] in good solvents, but the reduced strength parameter $B/2q$ (or $\lambda B$), which determines $\tilde{z}$ at a given $\lambda L$ (= $n_K$), is only 0.032 for the former and 1 order of magnitude smaller

than the latter group of systems because of the high stiffness of the CTDC chain. This small $B/2q$ for CTDC in NMP is responsible for the excluded-volume effects (on both $\langle S^2\rangle_z$ and $[\eta]$) that remain small up to as large an $n_K$ as 40.

## Conclusions

We have investigated 19 narrow-distribution fractions of cellulose tris[(3,5-dimethylphenyl)carbamate] ranging in $M_w$ from $2.5 \times 10^4$ to $7.5 \times 10^6$ by light scattering, sedimentation equilibrium, and viscometry in 1-methyl-2-pyrrolidone at 25 °C and analyzed the results together with our previous data on the basis of the Kratky−Porod wormlike chain with and without excluded volume. The major conclusions from this work may be summarized as follows.

1. The previous and present data for $\langle S^2\rangle_z$, $\delta$, and $[\eta]$ are described accurately by the known theories[19,21,29] for the unperturbed wormlike chain with a persistence length of 7.8 nm, a monomeric projection of 0.52 nm, an apparent polarizability parameter of −2.7, and a bead diameter of 3.9 nm if $M_w$ is lower than $7 \times 10^5$.

2. Excluded-volume effects on $\langle S^2\rangle_z$ and $[\eta]$ are appreciable for $M_w > 10^6$, i.e., for $n_K$ (the Kuhn segment number) > 50. This finding is consistent with Norisuye and Fujita's estimate[2] of the critical chain length for the onset of the experimentally observable volume effect in semiflexible polymer solutions.

3. Though it is seemingly inconsistent with the Yamakawa−Stockmayer−Shimada theory,[5−7] the theoretically predicted volume effects on both $\langle S^2\rangle$ and $[\eta]$ are sufficiently small for $n_K$ below 40, and the molecular weight dependences of measured $\langle S^2\rangle_z$ and $[\eta]$ are indeed explained quantitatively in the YSS theoretical framework, i.e., by the YSS theory combined with the Domb−Barrett function[8] for $\alpha_S^2$ or the Barrett function[35] for $\alpha_\eta^3$. The last conclusion suggests that the YSS theory should be applicable to moderately stiff chains as well as flexible and weakly stiff polymers.

**Acknowledgment.** This work was supported by a Grant-in-Aid (06403027) for Scientific Research from the Ministry of Education, Science and Culture, Japan.

## References and Notes

(1) Kratky, O.; Porod, G. *Recl. Trav. Chim. Pays-Bas* **1949**, *68*, 1106.
(2) Norisuye, T.; Fujita, H. *Polym. J.* **1982**, *14*, 143.
(3) Fujita, H. *Macromolecules* **1988**, *21*, 179.
(4) Yamakawa, H. In *Molecular Conformation and Dynamics of Macromolecules in Condensed Systems*; Nagasawa, M., Ed.; Elsevier: Amsterdam, 1988; p 21.
(5) Yamakawa, H.; Stockmayer, W. H. *J. Chem. Phys.* **1972**, *57*, 2843.
(6) Yamakawa, H.; Shimada, J. *J. Chem. Phys.* **1985**, *83*, 2607.
(7) Shimada, J.; Yamakawa, H. *J. Chem. Phys.* **1986**, *85*, 591.
(8) Domb, C.; Barrett, A. J. *Polymer* **1976**, *17*, 179.
(9) Kitagawa, T.; Sadanobu, J.; Norisuye, T. *Macromolecules* **1990**, *23*, 602.
(10) Abe, F.; Einaga, Y.; Yoshizaki, T.; Yamakawa, H. *Macromolecules* **1993**, *26*, 1884.
(11) Abe, F.; Einaga, Y.; Yamakawa, H. *Macromolecules* **1993**, *26*, 1891.
(12) Abe, F.; Horita, K.; Einaga, Y.; Yamakawa, H. *Macromolecules* **1994**, *27*, 725.
(13) Kamijo, M.; Abe, F.; Einaga, Y.; Yamakawa, H. *Macromolecules* **1995**, *28*, 1095.
(14) Murakami, H.; Norisuye, T.; Fujita, H. *Macromolecules* **1980**, *13*, 345.
(15) Tsuboi, A.; Yamasaki, M.; Norisuye, T.; Teramoto, A. *Polym. J.* **1995**, *27*, 1219.
(16) Rubingh, D. N.; Yu, H. *Macromolecules* **1976**, *9*, 681.
(17) Berry, G. C. *J. Chem. Phys.* **1966**, *44*, 4550.
(18) Yamakawa, H. *Modern Theory of Polymer Solutions*; Harper & Row: New York, 1971.
(19) Nagai, K. *Polym. J.* **1972**, *3*, 67.
(20) Yamakawa, H.; Fujii, M.; Shimada, J. *J. Chem. Phys.* **1979**, *71*, 1611.
(21) Benoit, H.; Doty, P. *J. Phys. Chem.* **1953**, *57*, 958.
(22) Carlson, C. W.; Flory, P. J. *J. Chem. Soc., Farady Trans. II* **1977**, *73*, 1505.
(23) Suter, U. W.; Flory, P. J. *J. Chem. Soc., Farady Trans. II* **1977**, *73*, 1521.
(24) Konishi, T.; Yoshizaki, T.; Shimada, J.; Yamakawa, H. *Macromolecules* **1989**, *22*, 1921.
(25) Flory, P. J. *Statistical Mechanics of Chain Molecules*; Wiley: New York, 1969.
(26) Sakurai, K.; Ochi, K.; Norisuye, T.; Fujita, H. *Polym. J.* **1984**, *16*, 559.
(27) Noordermeer, J. W. M.; Daryanani, R.; Janeschitz-Kriegl, H. *Polymer* **1975**, *16*, 359.
(28) Tsvetkov, V. N.; Andreeva, L. N. *Adv. Polym. Sci.* **1981**, *39*, 95.
(29) Yoshizaki, T.; Nitta, I.; Yamakawa, H. *Macromolecules* **1988**, *21*, 165.
(30) Takahashi, Y. *Macromolecules* **1991**, *24*, 3968.
(31) Zugenmaier, P.; Vogt, U. *Makromol. Chem.* **1983**, *184*, 1749.
(32) Steinmeier, H.; Zugenmaier, P. *Carbohydr. Res.* **1987**, *164*, 97.
(33) Yamakawa, H.; Fujii, M. *Macromolecules* **1974**, *7*, 128.
(34) Yamakawa, H.; Yoshizaki, T. *Macromolecules* **1980**, *13*, 633.
(35) Barrett, A. J. *Macromolecules* **1984**, *17*, 1566.
(36) Hayashi, K.; Tsutsumi, K.; Nakajima, F.; Norisuye, T.; Teramoto, A. *Macromolecules* **1995**, *28*, 3824.
(37) Akasaka, K.; Nakamura, Y.; Norisuye, T.; Teramoto, A. *Polym. J.* **1994**, *26*, 1387.

MA951344Q